Rapid Communications

Spin accumulation induced by a singlet supercurrent

Morten Amundsen and Jacob Linder
Center for Quantum Spintronics, Department of Physics, Norwegian University of Science and Technology, NO-7491 Trondheim, Norway

(Received 19 February 2020; revised 9 September 2020; accepted 11 September 2020; published 28 September 2020)

We show that a supercurrent carried by spinless singlet Cooper pairs can induce a spin accumulation in the normal metal interlayer of a Josephson junction. This phenomenon occurs when a nonequilibrium spin-energy mode is excited in the normal metal, for instance, by an applied temperature gradient between ferromagnetic electrodes. Without supercurrent, the spin accumulation vanishes in the Josephson junction. With supercurrent, a spatially antisymmetric spin accumulation is generated that can be measured by tunneling to a polarized detector electrode or by a nano-superconducting quantum interference device. We explain the physical origin of the induced spin accumulation by the combined effect of a Doppler shift induced by a flow of singlet Cooper pairs, and the spin-energy mode excited in the normal metal. This effect shows that spin control is possible even with singlet Cooper pairs in conventional superconductors, a finding which could open interesting perspectives in superconducting spintronics.

DOI: 10.1103/PhysRevB.102.100506

Introduction. Using superconductors to achieve interesting spin-dependent quantum effects is the central goal in the growing field of superconducting spintronics [1,2]. Despite the fact that superconductivity is usually antagonistic to magnetism, a series of experiments have in recent years proven that superconductors can be used to achieve phenomena such as long-ranged and dissipationless spin currents [3,4], large thermoelectric effects when combined with spin-polarized barriers [5], spin Hall signals exceeding the normal-state value by three orders of magnitude [6], and quantum phase batteries [7].

A key component of superconducting spintronics has traditionally been to find ways to generate polarized triplet Cooper pairs which can transport spin without resistance. In contrast, conventional superconductors described by Bardeen-Cooper-Schrieffer theory [8] are condensates of singlet Cooper pairs. While such condensates support supercurrents of charge, they do not generate supercurrents of spin. It might therefore seem as if supercurrents in conventional superconductors do not have much use in spintronics, where the aim is to control and detect spin-polarized signals [9].

Here, we show that supercurrents carried by singlet Cooper pairs can induce a spin accumulation in a normal metal despite the fact that they have no spin. This phenomenon occurs when a nonequilibrium spin-energy mode is excited in the normal metal. We show that the induced spin accumulation can be understood physically from the combined effect of a Doppler shift induced by the supercurrent and the existence of a spin-energy excitation in the normal metal. The fact that the spin accumulation can be controlled by a superflow of spinless Cooper pairs opens up for a different way in which conventional superconductors can merge with spintronics.

Results. The proposed setup for measuring this effect is shown in Fig. 1. Two thin normal metals are stacked on top of each other, creating a four-terminal device. Two ferromagnetic leads with antiparallel magnetizations are attached to opposite terminals, and superconducting leads are attached to the remaining two terminals, all of which forming tunneling contacts. When a supercurrent is passed through the superconducting electrodes, a spin accumulation is generated in the normal metal separating them. In the absence of supercurrent, the spin accumulation vanishes in the region between the superconductors. The length of each of the normal metals is assumed to be 3ξ, where ξ is the coherence length of the superconductors, which then gives the distance between opposite terminals. We assume that the system is in the diffusive limit, with a short mean free path. At the low temperatures relevant for superconductivity, inelastic electron-electron and electron-phonon scattering are suppressed [10], meaning that spin heat relaxation takes place mostly via elastic spin-flip scattering processes. Furthermore, the spin-flip scattering length is assumed to be longer than the size of the system, so that the spin diffusion in the normal metal is negligible. This is achievable, e.g., by using niobium superconductors, which have a coherence length of $\xi = 10$–15 nm in the diffusive limit, and copper normal metals, in which the spin diffusion length at low temperatures can be longer than 100 nm, even with a high concentration of impurities [11,12].

The physical mechanism behind this result can then be understood by the following simplified picture. Consider a ferromagnet–normal metal–ferromagnet (FNF) spin valve, with an antiparallel orientation of the magnetization in the ferromagnets. We increase the temperature of the right F by a certain amount ΔT relative to the temperature T_0 of the left F, thereby producing a gradient in the nonequilibrium effective temperature of the normal metal. The tunneling amplitude of particles at the F-N metal interfaces is higher when their spin is parallel to the magnetization than if it is antiparallel. The former is therefore influenced by a temperature increase in the F reservoir to a greater degree than the latter, leading to

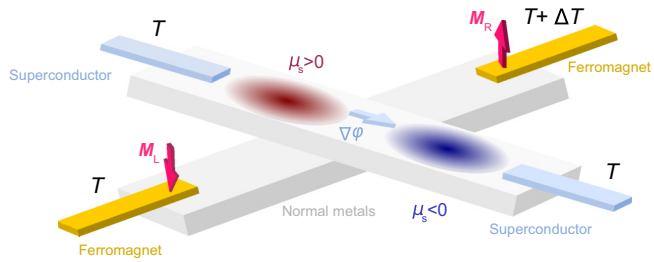

FIG. 1. Two superconducting electrodes (S) are deposited on top of a normal metal film (purple region). Far away from the superconducting electrodes, two antiparallel ferromagnets are in contact with the normal metal film. When a temperature gradient is applied between the ferromagnets, a spin-energy mode is excited throughout the normal metal. In the middle of the normal metal, between the superconductors, there exists no spin accumulation in the absence of a supercurrent. This corresponds to zero phase gradient across the Josephson junction, $\nabla\varphi = 0$. When a supercurrent is applied, $\nabla\varphi \neq 0$, an antisymmetric spin accumulation is induced in the normal metal between the superconductors.

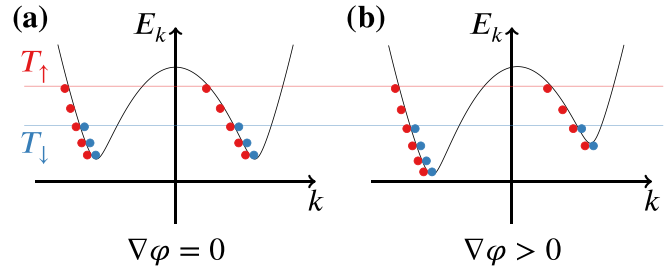

FIG. 2. Illustration of how a phase gradient in a superconductor leads to a spin imbalance when there is a gradient in the temperature difference $T_s = T_\uparrow - T_\downarrow$ between spin-up and spin-down particles. (a) The energy band of the superconductor when there is no phase gradient. The gradient ∇T_s breaks the balance between left- and right-moving quasiparticles. We show here the occupation of quasiparticles for $\nabla T_s < 0$ where for simplicity a scenario with only left-moving quasiparticle excitations is considered. (b) The same energy band when $\nabla\varphi > 0$. The resulting Doppler shift leads to a net spin imbalance, as the symmetry between left-moving electron and hole branches is now additionally broken.

a temperature difference between particles of opposite spin. The temperature on the right and left side of the normal metal for spin j, T_R^j and T_L^j, respectively, is then given as

$$T_R^\uparrow = T_0 + \left(1 - \frac{b}{2}\right)\Delta T, \tag{1}$$

$$T_R^\downarrow = T_0 + \left(1 - \frac{b}{2}\right)\Delta T - p(1-b)\Delta T, \tag{2}$$

$$T_L^\uparrow = T_0 + \frac{b}{2}\Delta T + p(1-b)\Delta T, \tag{3}$$

$$T_L^\downarrow = T_0 + \frac{b}{2}\Delta T, \tag{4}$$

where $b \in [0, 1]$ represents the thermal resistance independent of spin direction at the interface, and the polarization $p \in [0, 1]$ takes into account the spin-direction dependence of the tunneling. For $p = 0$, both spin species have identical temperature. For $p = 1$, $T_R^\downarrow$ and $T_L^\uparrow$ are completely insulated from the adjacent interface, and thus equilibrate to the temperature at the opposite end. The temperature distribution throughout the normal metal is simply given by

$$T^j(x) = \frac{1}{2}\left(T_R^j + T_L^j\right) + \left(T_R^j - T_L^j\right)\frac{x}{L}, \tag{5}$$

where L is the distance between the ferromagnets and $x \in (-L/2, L/2)$. The temperature difference T_s between spin-up and spin-down electrons then becomes

$$T_s(x) = T^\uparrow(x) - T^\downarrow(x) = p(1-b)\Delta T. \tag{6}$$

In other words, a spin valve in the antiparallel configuration gives a spatially constant temperature difference between electrons of opposite spin. We emphasize that while this is a phenomenological model, it can be derived from the quasiclassical theory employed in producing the main results of this Rapid Communication, as shown in Ref. [13], in the linear regime of a small ΔT.

When the superconducting leads are added to the spin valve as shown in Fig. 1, the picture is modified. Consider first a bulk ballistic superconducting material, with a band structure as shown in Fig. 2. If the superconductor experiences a constant T_s, then spin-up quasiparticles generally have higher excitation energies, but there are just as many electronlike excitations as there are holelike—all four branches are equally occupied, and so there is no spin accumulation. In contrast, a gradient in T_s leads to an uneven occupation of the branches. This is illustrated in Fig. 2(a) for $\nabla T_s < 0$. For simplicity, an extreme case is shown, where the gradient is so large that only the electronlike branch at $k < 0$, and the holelike branch at $k > 0$ are occupied. This is, however, still not enough to produce a spin accumulation, due to the balance of electronlike and holelike excitations. The final, necessary ingredient is a phase gradient $\nabla\varphi$ parallel to ∇T_s. In that case, a Doppler shift of the energy band is created, reducing the gap for $k < 0$, and vice versa, as shown in Fig. 2(b). This leads to an imbalance between spin-up and spin-down quasiparticles, resulting in a spin accumulation.

The numerical simulations of the diffusive system perfectly corroborate the ballistic band-structure analysis presented in Fig. 2. At first sight this seems strange, as rampant scattering would average out any asymmetry of the band structure in momentum space. However, a reasonable explanation is that in a proximitized normal metal as considered here, the superconducting correlations in the normal metal decay away from the superconductors. In such an inhomogeneous, diffusive system, Fick's first law dictates that the quasiparticles, while behaving as random walkers, have a net drift towards lower particle density. Hence, they sample the band structure with a bias in the direction normal to the superconductor–normal metal interface. A phase difference between the superconductors provides a phase gradient which is parallel to this bias, and thus produces a Doppler shift in the gap induced by the superconducting correlations in the normal metal.

The inhomogeneous superconducting correlations in the normal metal have an additional effect. Since the Cooper pairs have a singlet spin structure, it is clear that the presence of such correlations has a detrimental effect on the spin

temperature. This decay in T_s is largest near the superconducting leads, where the superconducting correlations are greatest, and smallest near the center of the system. In other words, a gradient in the, otherwise constant, spin temperature is established when the superconducting leads are attached.

To summarize, the simplified analysis above implies the generation of a spin accumulation in the system shown in Fig. 1. The role of the singlet superconductors is twofold. First, they introduce a transversal variation (in the direction between the superconductors) to an otherwise constant temperature difference between spin-up and spin-down particles. Second, when a phase gradient is applied, which will be parallel to ∇T_s, a net spin imbalance is produced. To prove this, we have to consider both the superconducting correlations induced in the normal metal due to the proximity effect as well as the nonequilibrium population of quasiparticles caused by the temperature gradient applied across the normal metal. A suitable theoretical framework for this purpose is the Keldysh-Usadel theory for nonequilibrium Green's functions [14,15]. In recent years, this formalism has been used to predict several interesting phenomena in superconducting hybrid structures driven out of equilibrium [16–20]. This theory is valid in the diffusive regime of transport, where impurity scattering randomizes the momentum of quasiparticles, in which case the Green's function matrix in the normal metal can be obtained by solving the Usadel equation,

$$D\nabla \cdot \check{g}\nabla\check{g} + i[\varepsilon\check{\rho}_4, \check{g}] = 0, \tag{7}$$

where D is the diffusion constant and ε is the quasiparticle energy. We note that the Usadel equation takes the form of a diffusion equation, and Fick's first law, which describes the net particle drift in an inhomogeneous system, is given as $\boldsymbol{J} = -D\check{g}\nabla\check{g}$. The Green's function matrix has the structure

$$\check{g} = \begin{pmatrix} \hat{g}^R & \hat{g}^K \\ 0 & \hat{g}^A \end{pmatrix}, \tag{8}$$

in Keldysh space, where $\hat{g}^X$ are 4×4 matrices in particle-hole and spin space. Furthermore, we have $\check{\rho}_4 = \mathrm{diag}(\hat{\rho}_4, \hat{\rho}_4)$, with $\hat{\rho}_4 = \mathrm{diag}(+1, +1, -1, -1)$. The retarded and advanced Green's functions $\hat{g}^R$ and $\hat{g}^A$ determine the band structure of the system, and these components satisfy an equation which is identical in form to Eq. (7). The quasiparticle excitations are determined by the Keldysh Green's function $\hat{g}^K$. Without loss of generality, this matrix can be parametrized as $\hat{g}^K = \hat{g}^R\hat{h} - \hat{h}\hat{g}^A$, where $\hat{h}$ is a distribution function. Its matrix structure in particle-hole and spin space can be further parametrized as

$$\hat{h} = \sum_n h_n\hat{\rho}_n, \tag{9}$$

where $\hat{\rho}_0 = \hat{I}$, $\hat{\rho}_j = \hat{\sigma}_j$, and $\hat{\rho}_{4+j} = \hat{\rho}_4\hat{\rho}_j$ for $j \in \{1, 2, 3\}$. The matrix $\hat{I}$ is the identity, and $\hat{\sigma}_j = \mathrm{diag}(\sigma_j, \sigma_j^*)$ for the Pauli matrix σ_j. In the following, we assume that both ferromagnets are aligned in the z direction, in which case the only relevant distribution functions become h_0, h_3, h_4, and h_7. Insertion into Eq. (7) gives

$$a_{mn}\nabla^2 h_n + \boldsymbol{b}_{mn}\cdot\nabla h_n = 0, \tag{10}$$

where $a_{mn} = D\,\mathrm{Tr}[\hat{\rho}_m\hat{\rho}_n - \hat{\rho}_m\hat{g}^R\hat{\rho}_n\hat{g}^A]/4$, and $\boldsymbol{b}_{mn} = \nabla a_{mn} + D\,\mathrm{Tr}[\hat{\rho}_n\hat{\rho}_m\hat{g}^R\nabla\hat{g}^R - \hat{\rho}_m\hat{\rho}_n\hat{g}^A\nabla\hat{g}^A]/4$. The function h_0 is the energy mode, and gives the temperature distribution of the system, with $h_0 = \tanh\frac{\varepsilon}{2k_BT}$, where k_B is the Boltzmann constant, being the only nonzero component of $\hat{h}$ in equilibrium. h_3 is a spin-energy mode. It can be related to an effective temperature difference between spin-up and spin-down quasiparticles via the Sommerfeld expansion [21,22], in a similar fashion as shown in Ref. [13]. The charge mode h_4 gives the quasiparticle charge distribution in the system, and the spin mode h_7 gives the magnetization, through the relation

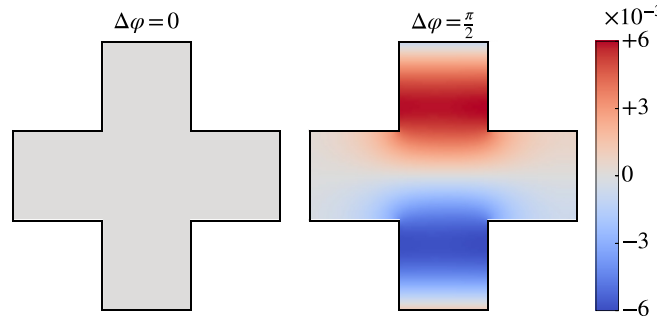

FIG. 3. Numerical simulations of the magnetization induced by the spin accumulation, scaled by M_0, in the presence of a temperature gradient. The superconducting terminals (top and bottom), and the left ferromagnet have a temperature of $T_l = 0.1T_c$, whereas the right ferromagnet has a temperature of $T_h = 0.5T_c$. No magnetization is induced when $\Delta\varphi = 0$.

$$M_s(\boldsymbol{r}) = M_0\int_{-\infty}^{\infty} ds\, h_7(s,\boldsymbol{r})\nu(s,\boldsymbol{r}). \tag{11}$$

In Eq. (11), we have neglected any triplet superconducting correlations, as is the case in our system, which would otherwise also give a contribution. Furthermore, $\nu(\varepsilon,\boldsymbol{r})$ is the local density of states, and $M_0 = g\mu_B\nu_0\Delta/4$, where g is the Landé g-factor, μ_B is the Bohr magneton, and ν_0 is the density of states of the normal metal, at the Fermi level. Using typical values of $\nu_0 \sim 10^{28}\ \mathrm{eV}^{-1}\,\mathrm{m}^{-3}$ and $\Delta \sim 10^{-3}$ eV, this gives $M_0 \sim 10^2$ A/m.

To describe the interfaces to the reservoirs, we use a generalization of the Kupriyanov-Lukichev tunneling boundary conditions, which take spin polarization into account [23,24],

$$2\zeta\hat{n}\cdot\check{g}\nabla\check{g} = [\check{g},\check{g}'] + \zeta_{mr}[\check{g},\{\check{\sigma}_3,\check{g}'\}] + \zeta_1[\check{g},\check{\sigma}_3\check{g}'\check{\sigma}_3], \tag{12}$$

where $\hat{n}$ is the interface normal, $\zeta = \rho/\rho_c$, with ρ the resistivity of the normal metal and ρ_c the contact resistivity, and $\check{g}'$ is the reservoir Green's function. The parameters $\zeta_{mr} = P/(1+\sqrt{1-P^2})$ and $\zeta_1 = (1-\sqrt{1-P^2})/(1+\sqrt{1-P^2})$ give the spin filtering at the interface, for a given polarization P. For interfaces to the ferromagnets, we set $\zeta = 3$ and $P = 0.6$, whereas for the superconductors, we set $\zeta = 1$ and $P = 0$. To generate a temperature gradient in the normal metal, we set the temperature in the left ferromagnetic reservoir, as well as in the two superconducting leads to be $T_l = 0.1T_c$, and the temperature in the right ferromagnetic reservoir to be $T_h = 0.5T_c$. The retarded and advanced components of Eq. (7), and subsequently Eq. (10), are solved using the finite-element method [25], and the resulting magnetization is computed using Eq. (11). The results are shown in Fig. 3. It is seen that when the phase difference $\Delta\varphi$ is zero, no magnetization is

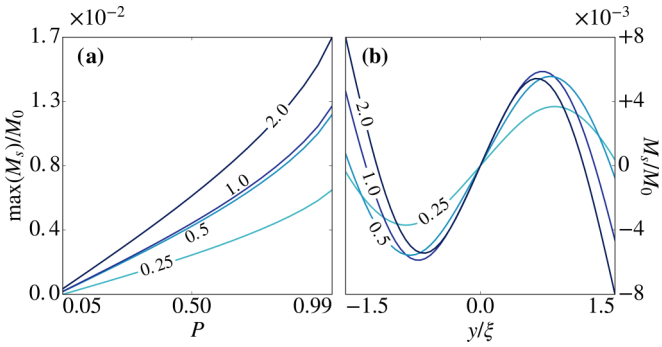

FIG. 4. The effect of varying the temperature in the right ferromagnetic reservoir. (a) shows the maximum magnetization as a function of the interface polarization P, and (b) shows the distribution of the magnetization along a coordinate y moving in a straight line between the superconductors. The annotations denote different T_h/T_c, and $\max(M_s)$ is the magnetization located along y.

induced in the normal metal. In stark contrast, an antisymmetric magnetization appears when $\Delta\varphi = \pi/2$. Thus, a supercurrent carried by spinless Cooper pairs induces a magnetization.

A magnetization can also be generated due to the presence of the ferromagnets, which in proximity to a superconductor can produce triplet superconducting correlations [26]. Another source of triplet correlations is the spin filtering at the interfaces, which would polarize the supercurrent if it detours via the ferromagnets on its way from one superconducting lead to the other. However, for the present geometry, the ferromagnets are located sufficiently far away from the superconducting leads that these mechanisms can be disregarded. In other words, the triplet superconducting correlations are completely negligible in this system, and the magnetization is induced solely by the interaction between the singlet (spin-0) Cooper pairs and the nonequilibrium temperature distribution. The heat injection may also cause a spin accumulation via the spin-dependent Seebeck effect [10,27], which is not captured by the quasiclassical formalism employed herein. Such an effect is, however, independent of the superconducting phase gradient, and hence not of interest in the present study.

From Fig. 4 it is seen that the induced magnetization is on the order of $M_s \sim 10^{-2} M_0 \sim 1$ A/m, which is equivalent to a spin accumulation on the order of 10^{-5} eV. This may be measured by attaching a ferromagnetic contact to the region of highest spin accumulation, and measuring the potential as a function of the orientation of the contact magnetization, in a similar way as was done in Ref. [27]. Alternatively, the spin accumulation generates a magnetic flux density on the order of $\mu_0 M_s \sim 10^{-6}$ T. This is well within the sensitivity of an AC nano-superconducting quantum interference device (SQUID), which can reach 50 nT [28]. Furthermore, this approach has the advantage of isolating the signal due to the singlet spin accumulation. Indeed, since all other contributions are independent of the phase difference between the superconducting leads, an AC magnetic field solely due to the spin accumulation can be generated by varying the phase difference with a controllable frequency, e.g., through an AC current source. It is interesting to investigate how the induced magnetization depends on the system parameters. In Fig. 4(a) we show the maximum magnetization as a function of the interface polarization P, for a variety of different temperature gradients. Polarizations up to 90% can be obtained, e.g., by replacing the ferromagnetic reservoirs in Fig. 1 with normal reservoirs that couple to the central normal metal via a ferromagnetic insulator such as EuS [29]. It is seen that the magnetization increases with P, and that this increase is steeper for higher T_h. This result is reasonable, as both parameters combined generate an effective spin temperature difference T_s, in correspondence with Eq. (6). Figure 4(b) shows the distribution of the magnetization along a straight line between the superconducting leads. For a low-temperature difference $T_h - T_l$, the largest magnetization takes place about halfway between the center of the system and the superconductors. However, as T_h increases these maxima are eventually overtaken by a larger magnetization at the superconductor interfaces. This is likely because of the increasing temperature gradient between the right ferromagnet and the superconductors, which leads to an increasing heat exchange between the two. Since the temperature in the latter is spin independent, this serves to mollify the effective spin temperature difference T_s near the superconductors, and thus increase the gradient in h_3. This, in turn, leads to a higher magnetization when a phase gradient is applied. We note, however, that these results are obtained while assuming the superconductors act as temperature reservoirs. A continued increase in T_h will likely invalidate this assumption, and lead to a saturation of the induced magnetization. We also note that a spin-heat accumulation, described by a finite h_3 and T_s, should in general also occur close to the interface on the ferromagnetic side [30].

Finally, we remark that it is also possible to generate a spin-dependent temperature difference by applying a voltage bias between the ferromagnets, rather than a temperature gradient. In this case, the largest average T_s in the system would be obtained for a parallel alignment of the ferromagnets. A phase gradient between the superconducting leads will then produce a spin accumulation by the same mechanism as previously described. However, in addition to providing a T_s, the injected quasiparticles also lead to a spin imbalance, and thus directly contribute to the spin accumulation. This additional contribution to the spin accumulation would be independent of the phase gradient, and hence it would still be possible to isolate the signal due to the singlet superconducting correlations also in this case.

Conclusion. We have shown that a supercurrent carried by spinless Cooper pairs can induce a spin accumulation in a normal metal. This is possible when a spin-energy distribution mode is excited in the normal metal out of equilibrium, which allows a spin accumulation to arise due to the Doppler shift caused by the supercurrent in the quasiparticle energies. Our finding shows that spin control is possible even with singlet Cooper pairs in conventional superconductors, which could open interesting avenues for further research in superconducting spintronics.

Acknowledgments. We thank T. T. Heikkilä for helpful comments, and J. W. Wells for useful discussions. M.A. and J.L. were supported by the Faculty of Sciences, NTNU, and the Centres of Excellence funding scheme from the Research Council of Norway, Grant No. 262633 *QuSpin*. We thank J. A. Ouassou for useful discussions.

[1] J. Linder and J. W. A. Robinson, Nat. Phys. **11**, 307 (2015).
[2] M. Eschrig, Rep. Prog. Phys. **78**, 104501 (2015).
[3] J. W. A. Robinson, J. D. S. Witt, and M. G. Blamire, Science **329**, 59 (2010).
[4] T. S. Khaire, M. A. Khasawneh, W. P. Pratt, Jr., and N. O. Birge, Phys. Rev. Lett. **104**, 137002 (2010).
[5] S. Kolenda, M. J. Wolf, and D. Beckmann, Phys. Rev. Lett. **116**, 097001 (2016).
[6] T. Wakamura, Y. Akaike, Y. Omori, Y. Niimi, S. Takahashi, A. Fujimaki, S. Maekawa, and Y. Otani, Nat. Mater. **14**, 675 (2015).
[7] D. B. Szombati, S. Nadj-Perge, D. Car, S. R. Plissard, E. P. A. M. Bakkers, and L. P. Kouwenhoven, Nat. Phys. **12**, 568 (2016).
[8] J. Bardeen, L. N. Cooper, and J. R. Schrieffer, Phys. Rev. **108**, 1175 (1957).
[9] I. Zutic, J. Fabian, and S. Das Sarma, Rev. Mod. Phys. **76**, 323 (2004).
[10] G. E. W. Bauer, E. Saitoh, and B. J. van Wees, Nat. Mater. **11**, 391 (2012).
[11] J. Bass and W. P. Pratt, Jr., J. Phys.: Condens. Matter **19**, 183201 (2007).
[12] Q. Fowler, B. Richard, A. Sharma, N. Theodoropoulou, R. Loloee, W. P. Pratt, Jr., and J. Bass, J. Magn. Magn. Mater **321**, 99 (2009).
[13] See Supplemental Material at http://link.aps.org/supplemental/10.1103/PhysRevB.102.100506 for a derivation of the effective temperature distribution from quasiclassical theory.
[14] K. Usadel, Phys. Rev. Lett. **25**, 507 (1970).
[15] J. Rammer and H. Smith, Rev. Mod. Phys. **58**, 323 (1986).
[16] D. Beckmann, J. Phys.: Condens. Matter **28**, 163001 (2016).
[17] F. S. Bergeret, M. Silaev, P. Virtanen, and T. T. Heikkilä, Rev. Mod. Phys. **90**, 041001 (2018).
[18] D. S. Rabinovich, I. V. Bobkova, A. M. Bobkov, and M. A. Silaev, Phys. Rev. Lett. **123**, 207001 (2019).
[19] F. Aikebaier, M. A. Silaev, and T. T. Heikkilä, Phys. Rev. B **98**, 024516 (2018).
[20] T. T. Heikkilä, M. Silaev, P. Virtanen, and F. S. Bergeret, Prog. Surf. Sci. **94**, 100540 (2019).
[21] T. T. Heikkilä, M. Hatami, and G. E. W. Bauer, Phys. Rev. B **81**, 100408(R) (2010).
[22] N. Ashcroft and N. Mermin, *Solid State Physics* (Brooks/Cole Cengage Learning, Boston, 1976).
[23] M. Yu. Kupriyanov and V. F. Lukichev, Sov. Phys. JETP **67**, 1163 (1988).
[24] M. Eschrig, A. Cottet, W. Belzig, and J. Linder, New J. Phys. **17**, 083037 (2015).
[25] M. Amundsen and J. Linder, Sci. Rep. **6**, 22765 (2016).
[26] A. I. Buzdin, Rev. Mod. Phys. **77**, 935 (2005).
[27] A. Slachter, F. L. Bakker, J.-P. Adam, and B. J. van Wees, Nat. Phys. **6**, 879 (2010).
[28] D. Vasyukov, Y. Anahory, L. Embon, D. Halbertal, J. Cuppens, L. Neeman, A. Finkler, Y. Segev, Y. Myasoedov, M. L. Rappaport, M. E. Huber, and E. Zeldov, Nat. Nanotechnol. **8**, 639 (2013).
[29] N. Müller, W. Eckstein, W. Heiland, and W. Zinn, Phys. Rev. Lett. **29**, 1651 (1972).
[30] F. K. Dejene, J. Flipse, G. E. W. Bauer, and B. J. van Wees, Nat. Phys. **9**, 636 (2013).